Available online at www.sciencedirect.com
SCIENCE DIRECT®
International Journal of Solids and Structures 43 (2006) 2318–2335
INTERNATIONAL JOURNAL OF SOLIDS and STRUCTURES
www.elsevier.com/locate/ijsolstr

Influence of temperature and strain rate on the mechanical behavior of three amorphous polymers: Characterization and modeling of the compressive yield stress

J. Richeton [a], S. Ahzi [a,*], K.S. Vecchio [b], F.C. Jiang [b], R.R. Adharapurapu [b]

[a] *Institut de Mécanique des Fluides et des Solides—UMR 7507, Université Louis Pasteur/CNRS, 67000 Strasbourg, France*
[b] *Materials Science and Engineering Program, University of California—San Diego, La Jolla, CA 92093-0411, USA*

Received 3 January 2005; received in revised form 16 June 2005
Available online 10 August 2005

Abstract

Uniaxial compression stress–strain tests were carried out on three commercial amorphous polymers: polycarbonate (PC), polymethylmethacrylate (PMMA), and polyamideimide (PAI). The experiments were conducted under a wide range of temperatures (−40 °C to 180 °C) and strain rates (0.0001 s^{-1} up to 5000 s^{-1}). A modified split-Hopkinson pressure bar was used for high strain rate tests. Temperature and strain rate greatly influence the mechanical response of the three polymers. In particular, the yield stress is found to increase with decreasing temperature and with increasing strain rate. The experimental data for the compressive yield stress were modeled for a wide range of strain rates and temperatures according to a new formulation of the cooperative model based on a strain rate/temperature superposition principle. The modeling results of the cooperative model provide evidence on the secondary transition by linking the yield behavior to the energy associated to the β mechanical loss peak. The effect of hydrostatic pressure is also addressed from a modeling perspective.

Keywords: Yield stress; Mechanical response; PC; PMMA; PAI; Amorphous polymers; Strain rate effect; Temperature effect; Pressure effect; Experiments; Modeling

* Corresponding author. Tel.: +33 3902 42952; fax: +33 3886 14300.
E-mail address: ahzi@imfs.u-strasbg.fr (S. Ahzi).

0020-7683/$ - see front matter © 2005 Elsevier Ltd. All rights reserved.
doi:10.1016/j.ijsolstr.2005.06.040

1. Introduction

Strain rate and temperature are known to significantly influence the mechanical behavior of polymers. Since the beginning of polymer science, numerous experimental studies have been carried out on polymers to characterize the mechanical behavior as a function of temperature and strain rate. Among these studies, a great deal of attention has been given to the yield stress. Bauwens-Crowet, Bauwens and co-workers (Bauwens-Crowet et al., 1969, 1972; Bauwens, 1972; Bauwens-Crowet, 1973) have studied the yield stress of PC, PMMA and PVC as a function of temperature and strain rate. In their work, they correlated the yield behavior with molecular processes such as the secondary relaxation, but they did not study the flow stress for strain rates higher than $1\ s^{-1}$. In particular, to test materials under dynamic loading, one common technique employed is the split-Hopkinson pressure bar. The theory and practical application of the split-Hopkinson pressure bar testing method are clearly presented and reviewed by Gray (2000) in the ASM—Handbook, Volume 8 "Mechanical Testing and Evaluation". The specific use of the split-Hopkinson pressure bar for the evaluation of the high strain rate deformation of polymers and other soft materials is critiqued by Gray and Blumenthal (2000). The first work on the high rate response of plastics is due to Kolsky (1949) wherein he identified the importance of sample thickness on the measured response of the polymers. Walley et al. (1989) compiled reviews on the high strain rate studies of polymers, and they also showed that the strain hardening behavior of glassy polymers is dependent on the strain rate and temperature. Chou et al. (1973) analyzed the compressive behavior of several plastics and concluded that the temperature rise developed during deformation cannot be neglected. They also observed that the yield strength increases with increasing strain rate. Similar results for the flow stress were also found by Briscoe and Nosker (1985).

While numerous studies have investigated the influence of strain rate on the constitutive response for several polymers at room temperature, the influence of temperature at high strain rate has received much less attention. Among these studies, Rietsch and Bouette (1990) studied the compression yield stress of PC over a wide range of temperatures and strain rates, and revealed the importance of the secondary transition to account for the flow stress increases. Later, Chen et al. (2002) showed that the dynamic stress–strain behavior under tension differs significantly from the dynamic compressive response. Blumenthal et al. (2002) examined the influence of both strain rate and temperature on the deformation response of PMMA and PC, and more recently, Cady et al. (2003) studied the mechanical response of several polymers under dynamic loading at high temperatures.

The aim of this paper is first to present experimental results illustrating the effect of strain rate and temperature on the mechanical response for three amorphous polymers (PC, PMMA and PAI) under a wide range of strain rates and temperatures. Both PC and PMMA are very common commercial products widely used for their optical and mechanical properties; these materials are also used in extreme temperature and loading condition such as impact-resistant aircraft windows. PAI is a high technology molding polymer for reliable performance at extremely high temperature and stress. Among the technologically advanced applications of PAI, it can be mentioned that parts of the space shuttle, automotive transmission, and many other critical components are molded from this polymer. The testing of these three materials for a wide range of strain rates and temperatures is a required step to develop constitutive modeling able to accurately predict the mechanical behavior for severe applications. This is why the second objective of this article is to model the compressive yield stresses according to the new formulation of the Eyring cooperative model as proposed by Richeton et al. (2005). At the end, we discuss how the effect of hydrostatic pressure can be incorporated in the proposed model.

2. Materials and experimental procedures

2.1. Materials

The materials used in this study were three amorphous polymers, polycarbonate (PC), polymethylmethacrylate (PMMA), and polyamideimide (PAI). Commercial grades of these materials were purchased as extruded rods from a local supplier under the trade names, GE Plastics Lexan® PC, Degussa AG Plexiglas® PMMA and Quadrant EPP Torlon® 4203 PAI.

2.2. Low strain rate compression testing

Quasi-static uniaxial compression tests were conducted on a servohydraulic Instron load frame. The samples were tested to large strains at different temperatures, ranging from −40 °C to temperatures above the glass transition temperature and at different constant extension rates, leading to strain rates ranging from 10^{-4} s^{-1} to 10 s^{-1}. Right cylindrical samples were machined to an aspect ratio of 1:1 from the extruded polymer rods. The exact dimensions of the specimens were of 6.35 mm in height and 6.35 mm in diameter. Grease was used between the sample end faces and the platens to minimize friction. Load data from the load cell and displacement data from the deflectometer were recorded using a data acquisition software. The corresponding true stress–true strain curves were computed and then plotted.

At low temperatures (−40 °C and 0 °C), tests were carried out in a methanol bath cooled down by liquid nitrogen, while at high temperatures the tests were conducted in a container filled with arachid oil heated up by a heating collar. In both cases, temperature was monitored through a K-type thermocouple and samples were held at temperature for approximately 5 min before starting the experiments.

2.3. High strain rate compression testing

Dynamic uniaxial compression tests were conducted for three different temperatures (−40 °C, 0 °C and 25 °C) at high strain rates of about 800–5000 s^{-1} using a split-Hopkinson pressure bar (SHPB) setup. The length of polymer samples used in high strain rate tests must be carefully chosen to ensure that stress equilibrium is achieved in the loading of the sample (Gray and Blumenthal, 2000). Following the guidelines from Gray and Blumenthal (2000) and more recently discussed in Cady et al. (2003), numerous preliminary tests were conducted on each of the three polymers tested here, to determine the maximum specimen length (l) to sample diameter (d) ratio that produced stress equilibrium throughout the tests. As a result of these preliminary tests, we verified the results of Cady et al. (2003), which indicated that an aspect ratio (l/d) equal to 1/2 will ensure stress equilibrium. The high strain rate specimen were machined to an (l/d) aspect ratio of 1/2 from the same polymer rods as for the low strain rate tests, and the exact dimensions of the specimens were of 3.18 mm in height and 6.35 mm in diameter. Grease was also used between the sample end faces and the platens to minimize friction. A schematic of the SHPB setup can be found in Fig. 1. The

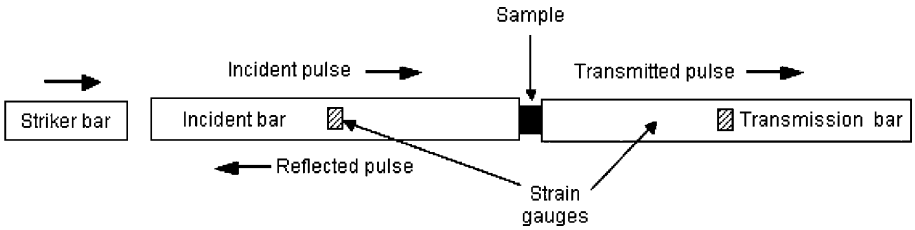

Fig. 1. Schematic representation of the SHPB setup.

sample is sandwiched between the incident bar and the transmitter bar, both of which are made out of C350 maraging steel. The striker bar (also made out of C350 maraging steel) is fired from a gas gun and impacts the incident bar to generate a pressure pulse, which travels down the incident bar and loads the sample. A portion of the incident pulse is reflected at the sample/bar interface, and the remaining part is transmitted through the sample into the transmission bar. In the present setup, the reflected pulse is measured, then captured in a momentum trap, and hence the sample is loaded only once. High gain, large band-width amplifiers were used to amplify the stress pulses traveling in the bars measured by strain gauges glued to the bars. The diameter of all the bars was 12.7 mm, the length of the striker bar was of 45.7 cm, and the incident and transmitter bars had the same length of 121.9 cm. The incident, reflected and transmitted pulse were recorded at a frequency of 10 MHz and were corrected for wave dispersion. Subsequently, the strain rate and true strain were calculated from the reflected pulse, and the sample true stress was calculated from the transmitted pulse. Furthermore, care was taken to verify that each tested sample was in stress equilibrium during the loading period of the test, and that a constant strain rate was achieved for the entire loading duration. Lastly, pulse shaping of the incident pulse was performed using a thin layer of petroleum jelly on the impact side of the incident bar. This thin layer of petroleum jelly has a distinct affect on reducing the inherent high-frequency noise associated with the impact generating the stress pulse, and increases the rise time of the incident pulse, which facilitates establishing stress equilibrium. Part of this noise inherent to dynamic loading was also attenuated from the stress–strain curves by realizing a numerical smoothening of experimental data. However any test wherein the sample was not under stress equilibrium, not deformed at a constant strain rate, or which produced a very noisy or oscillating transmitted pulse was discarded and not used in this study.

The SHPB tests were conducted at three temperatures: −40 °C, 0 °C and 25 °C. For the low temperatures, a methanol bath cooled down by liquid nitrogen was utilized. All the tests were repeated for several samples for each temperature and strain rate conditions. The quasi-static tests provided very good reproducibility, whereas a small variation in the stress–strain results was observed for dynamic tests.

3. Experimental results

3.1. Strain rate dependence

Fig. 2 presents the uniaxial compression true stress–true strain curves of PC, PMMA and PAI tested at 25 °C for various strain rates ranging from quasi-static to dynamic loadings. Only part of the experimental results is presented to ease the interpretation of the stress–strain curves. The first observation is that the yield stress increases with an increasing strain rate especially at high strain rates. Many authors (Bauwens, 1972; Bauwens-Crowet, 1973; Rietsch and Bouette, 1990; Xiao et al., 1994; Chen et al., 1999; Brulé et al., 2001; Rana et al., 2002; Richeton et al., 2005) believe that this increase of the yield stress is correlated to secondary molecular processes. An increasing strain rate will decrease the molecular mobility of the polymer chains by making the chains stiffer. A similar increase of the yield stress will be observed at the very low temperatures, where the yield stress dramatically increases with a decreasing temperature near the secondary relaxation temperature, T_β. The initial Young's modulus appears also to be strain rate dependent. In the case of PMMA and PAI, an increasing strain rate will noticeably increase the initial Young's modulus. This effect will have to be taken into account in the development of advanced models capable of predicting the mechanical properties of polymers under dynamic loading conditions.

Concerning the stress–strain behavior, all the three polymers exhibit a similar mechanical response at the low strain rates: first an initial elastic response followed by yielding, strain softening and then a dramatic strain hardening. The extent of strain softening depends on the material. For all three materials, the

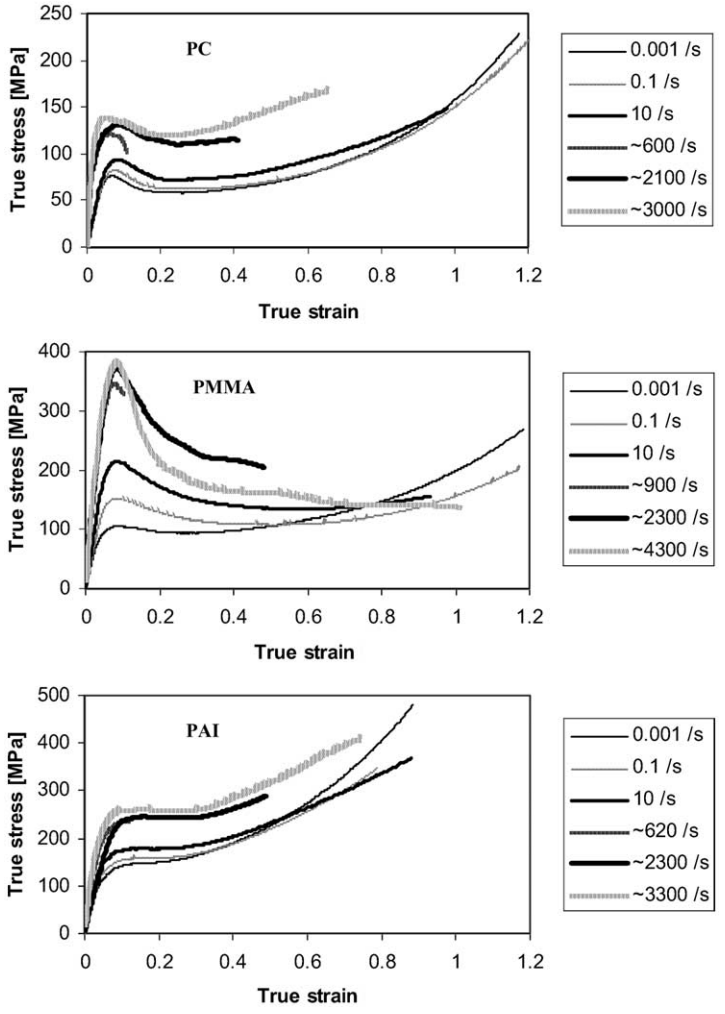

Fig. 2. Experimental uniaxial compression stress–strain curves for PC, PMMA and PAI at the temperature 25 °C over a wide range of strain rates.

adiabatic heating effect on the strain softening and the strain hardening cannot be neglected. This adiabatic temperature rise is easily recognizable in that at the large deformations the slope of the flow curve decreases (decreasing strain hardening rate) with an increasing strain rate. Generally this thermal effect becomes significant at the strain rate of 0.01 s^{-1}. Due to the low thermal diffusivities of polymers, effects of adiabatic heating are expected to be significant for high strain rate testing, yet still dependent on the polymer. The closer the adiabatic temperature rise approaches the glass transition temperature, the stronger the effect on the strain hardening rate. Indeed for PMMA, the strain hardening completely disappears at the high strain rates due to the adiabatic heating effect as shown in Fig. 2. Both PC and PAI show much less effect of the adiabatic heating on the strain hardening rate, yet the effect must still be incorporated into the constitutive model for these materials. The values of the glass transition temperature of the polymers can be found in Table 1.

Table 1
Parameters for the cooperative model

Parameters	PC	PMMA	PAI
n	5.88	6.37	6.58
V (m^3)	5.16×10^{-29}	5.14×10^{-29}	1.62×10^{-29}
$\sigma_i(0)$ (MPa)	145	190	315
m (MPa/K)	0.24	0.47	0.61
$\dot{\varepsilon}_0$ (s^{-1})	8.69×10^{12}	7.46×10^{15}	8.03×10^{11}
ΔH_β (kJ/mol)	40	90	25
T_g (K)	413	378	538
c_1^g	17.44	9.00	–
c_2^g (°C)	51.60	35.50	–

The WLF parameters of PC are from Ferry (1980) and those from PMMA are from Halary et al. (1991).

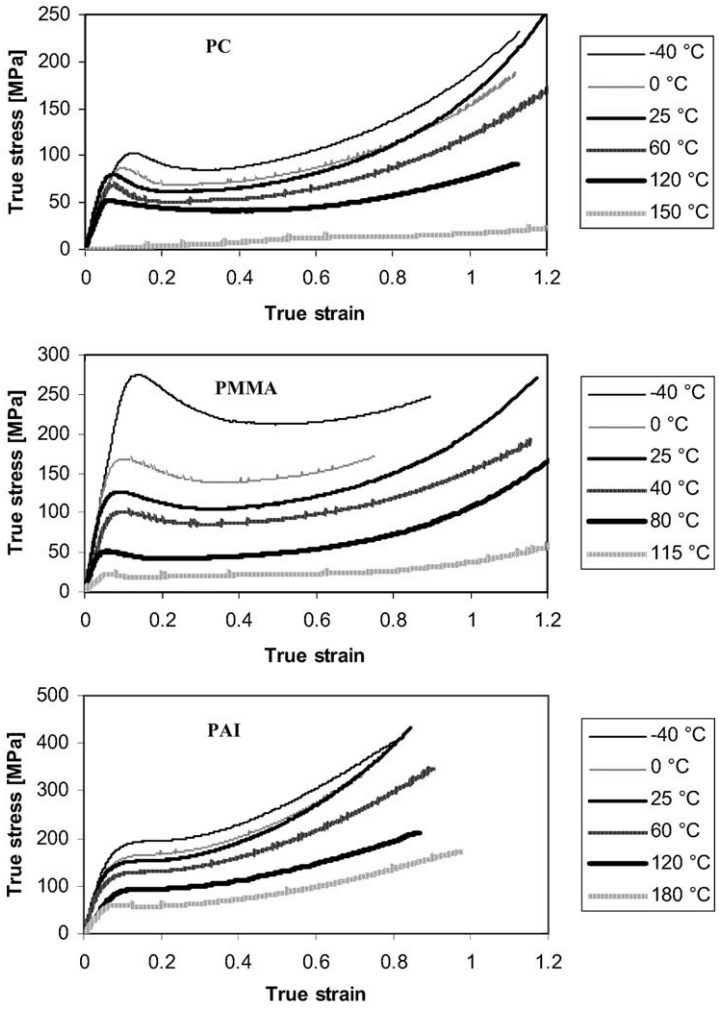

Fig. 3. Experimental uniaxial compression stress–strain curves for PC, PMMA and PAI at the strain rate of 0.01 s^{-1} over a wide range of temperature.

3.2. Temperature dependence

The compression true stress–true strain curves at a constant strain rate of 0.01 s^{-1} for various temperatures are given in Fig. 3. As expected the yield stress and the initial Young's modulus are found to decrease with an increasing temperature for all three materials; a similar effect is also observed for the strain hardening rate. This corroborates that the temperature rise at high strain rates controls the strain hardening rate, which depend itself on temperature. The closer the temperature is to the glass transition temperature, T_g, the lower the strain hardening rate. Strain hardening can even vanish for temperatures above T_g.

Concerning the yield stress, PMMA presents a significant increase for the low temperatures at −40 °C and 0 °C. The reason for this effect is that these low temperatures are below the secondary relaxation temperature of PMMA (about 10 °C). As is the case at high strain rates, the yield stress dramatically increases for temperatures below the secondary relaxation temperature, T_β. Here we can also mention that the PMMA samples tested at −40 °C and 0 °C, for the very high strain rates, fractured before yielding. When the theoretical yield stress value is superior to the brittle stress value, the polymer presents a brittle behavior. In the case of PMMA, the competition process between yielding and brittle failure cannot be neglected for the low temperatures and high strain rates. Similar increase of yield stress have also been observed for PC, where the yield stress of this material dramatically augments at about −100 °C/−150 °C (Boyer, 1968; Kastelic and Baer, 1973). According to Boyer (1968), this sharp increase in the yield point is associated with the β transition. This can easily be understood since below T_β the secondary molecular motions are restricted and thus the polymer chains are stiffer. Unfortunately for PAI, we could not find in the literature any data for the yield stress at very low temperatures or any values for the secondary transition temperature.

4. Modeling of the yield stress

4.1. Cooperative model

Many molecular theories have been proposed for the prediction of the yield stress of amorphous polymers (Eyring, 1936; Robertson, 1966; Bauwens-Crowet et al., 1969; Argon, 1973; Bowden and Raha, 1974). These theories consider the yield behavior as a thermally activated process and account for temperature and strain rate effects. Most of these models give an acceptable prediction for the yield stress, but only in a specific domain of temperatures and/or strain rates. In particular, Richeton et al. (2003) have revealed that these models are either unable to account for the dramatic increase of the yield stress at higher strain rates or non-valid in the glass transition temperature region. Recently, a new formulation of the Eyring cooperative model by Richeton et al. (2005) has shown to give satisfactory results for a wide range of strain rates and temperatures, including the high strain rates and the glass transition region.

The cooperative model is based on to the work of Fotheringham and Cherry (1976, 1978), where these authors have introduced the concept that yielding involves a cooperative motion of polymer chain segments to account for the significance of an activation volume during the yield process. They made two modifications to the original Eyring equation. First, they adopted a similar representation as in Haward and Thackray (1968), where it is assumed that there exists an internal stress, σ_i, that will reduce the effective stress, σ^*, defined by:

$$\sigma^* = \sigma_y - \sigma_i \tag{1}$$

This internal stress is a structural parameter, which provides a better way of expressing the observed macroscopic properties in polymeric materials. The value of σ_i is strongly affected by temperature. Second, they considered that the yield stress, σ_y, is obtained when many polymer chain segments are moving coopera-

tively at the same time. The resulting model is an Eyring-like equation, where the hyperbolic sine function is raised to an nth power.

$$\dot{\varepsilon} = \dot{\varepsilon}^* \sinh^n\left(\frac{(\sigma_y - \sigma_i)V}{2kT}\right) \tag{2}$$

Here, n is a material parameter used to characterize the cooperative movement of the chain segments, V is the activation volume, k is the Boltzmann constant and T is the absolute temperature. The characteristic strain rate, $\dot{\varepsilon}^*$, is thermally activated. The development of Richeton et al. (2005) consists of deriving the temperature dependence of $\dot{\varepsilon}^*$ and σ_i, so that both quantities conform to the strain rate/temperature superposition principle for the yield stress described by Bauwens-Crowet et al. (1969).

4.2. Strain rate/temperature superposition principle

It is well established that an increase in temperature will have the same effect on the yield stress as a decrease in strain rate. According to the well-known time-temperature superposition principle, which describes the equivalence of time (or frequency, herein assimilated as the strain rate) and temperature, the yield of amorphous polymers at low temperatures is comparable to that at high strain rates. Bauwens-Crowet et al. (1969) have established that the Eyring plots (curves representing σ_y/T versus $\log\dot{\varepsilon}$ for various temperatures) can be shifted to create a master curve for a given reference temperature, T_{ref}. Fig. 4 schematically illustrates the scaling properties of the Eyring plots where the shifts with respect to the master curve are both horizontal and vertical. The expression of these shifts is given by:

$$\begin{cases} \Delta(\log\dot{\varepsilon}) = \log\dot{\varepsilon}(T_{ref}) - \log\dot{\varepsilon}(T) \\ \Delta\left(\frac{\sigma_y}{T}\right) = \dfrac{\sigma_y(T_{ref})}{T_{ref}} - \dfrac{\sigma_y(T)}{T} \end{cases} \tag{3}$$

where $\Delta(\log\dot{\varepsilon})$ is the horizontal shift and $\Delta(\sigma_y/T)$ is the vertical shift. It needs to be pointed out that the strain rate, $\dot{\varepsilon}$, does not depend on the temperature; the form, $\dot{\varepsilon}(T)$, is only used for referencing the temperature at which the Eyring plot is represented.

Although, the scaling properties of the cooperative model have already been studied by Povolo and co-workers (Povolo and Hermida, 1995; Povolo et al., 1996), Richeton et al. (2005) have recently proposed a new development which assumes that, independent of the yield stress model, both of the horizontal and vertical shifts have to follow an Arrhenius-like temperature dependence. Subsequently, Richeton et al.

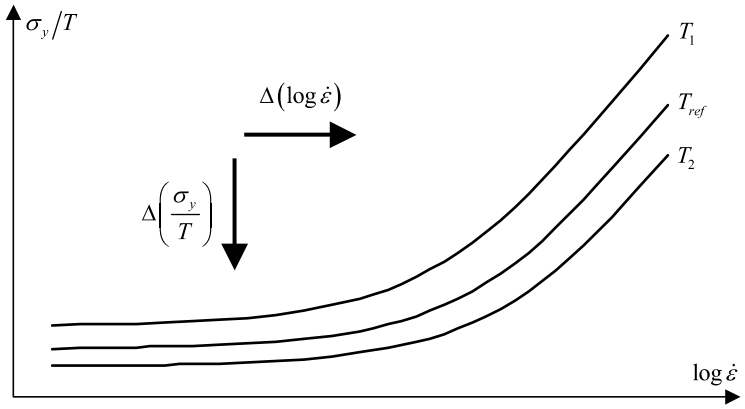

Fig. 4. Illustration of the strain rate—temperature superposition principle of the Eyring plots for three different temperatures $T_1 < T_{ref} < T_2$. The curves drawn for T_1 and T_2 can be superposed to the curve given for T_{ref}.

(2005) have drawn a parallel with the work of Bauwens (1972) and Bauwens-Crowet (1973) where the yield behavior has been linked with the β mechanical loss peak of the $T < T_g$ transition. As a matter of fact, the expressions of both shifts can be expressed as function of ΔH_β, the activation energy of the β loss peak. Finally according to these assumption, the expressions of $\dot{\varepsilon}^*$ and σ_i are derived as:

$$\begin{cases} \dot{\varepsilon}^*(T) = \dot{\varepsilon}_0 \exp\left(-\dfrac{\Delta H_\beta}{kT}\right) \\ \sigma_i(T) = \sigma_i(0) - mT \end{cases} \tag{4}$$

where $\dot{\varepsilon}_0$ is a constant pre-exponential strain rate, ΔH_β is the activation energy, $\sigma_i(0)$ is the athermal internal yield stress and m is a material parameter. Combining Eqs. (2) and (4), the expression of the yield stress is given by:

$$\sigma_y = \sigma_i(0) - mT + \frac{2kT}{V}\sinh^{-1}\left(\frac{\dot{\varepsilon}}{\dot{\varepsilon}_0 \exp\left(-\dfrac{\Delta H_\beta}{kT}\right)}\right)^{1/n} \tag{5}$$

4.3. Extension of the model through the glass transition region

Several authors such as Roetling (1965), Robertson (1966) and Bauwens et al. (1969) have previously studied and modeled the yield stress behavior of amorphous polymers through the glass transition region. For temperatures above T_g, it has been found that the yield stress vanishes to zero with respect to relations based on the concept of free volume. In the work of Richeton et al. (2005), the cooperative model was also extended through the glass transition according to the Williams–Landel–Ferry (WLF) equation (Ferry, 1980). In lines with the superposition principle between time (or frequency) and temperature, the WLF equation describes the mechanical properties of amorphous polymers in the range T_g to $T_g + 100$ °C. According to this development, the characteristic strain rate above T_g, $\dot{\varepsilon}^*(T \geqslant T_g)$, is be expressed as:

$$\dot{\varepsilon}^*(T \geqslant T_g) = \dot{\varepsilon}_0 \exp\left(-\frac{\Delta H_\beta}{kT_g}\right)\exp\left(\frac{\ln 10 \times c_1^g (T - T_g)}{c_2^g + T - T_g}\right) \tag{6}$$

where c_1^g and c_2^g are the WLF parameters and all other parameters have been defined previously. It can be noted that $\dot{\varepsilon}^*(T)$, as defined by Eq. (4) for $T < T_g$ and by Eq. (6) for $T \geqslant T_g$, is a continuous function of T.

For the determination of $\sigma_i(T \geqslant T_g)$, it was suggested by Fotheringham and Cherry (1976) to use a vanishing internal stress above T_g:

$$\sigma_i(T \geqslant T_g) = 0 \tag{7}$$

Heating an amorphous polymer above T_g must annihilate the past thermal history of the material. According to this assumption, the proposed model for the yield stress will not be continuous through the glass transition temperature region because the internal stress is inherently non-continuous. In addition the glass transition is postulated to occur for a single temperature. However it is universally known that it occurs for a large domain of temperature. Finally, by substituting Eqs. (6) and (7) into Eq. (2), the expression of the cooperative model above T_g is given by:

$$\sigma_y(T \geqslant T_g) = \frac{2kT}{V}\sinh^{-1}\left(\frac{\dot{\varepsilon}}{\dot{\varepsilon}_0 \exp\left(-\dfrac{\Delta H_\beta}{kT_g}\right)\exp\left(\dfrac{\ln 10 \times c_1^g (T - T_g)}{c_2^g + T - T_g}\right)}\right)^{1/n} \tag{8}$$

4.4. Physical nature of the model

Originally, Fotheringham and Cherry (1976, 1978), and Povolo and co-workers (Povolo and Hermida, 1995; Povolo et al., 1996) have not provided any information on the nature of the activation energy of the cooperative model. It is quite remarkable to notice that the β process is also involved in the cooperative process, since it is a physical process that has been identified as a plasticity precursor. It has been emphasized by Yee and co-workers (Xiao et al., 1994; Chen et al., 1999) and by Halary and co-workers (Brulé et al., 2001; Rana et al., 2002) that there exists a correlation between yielding and segmental mobility associated to the β relaxation processes (localized molecular motions). Therefore the curvature of the Eyring plots at high strain rates and at low temperatures may also be accounted for by the existence of this secondary transition.

Concerning the internal stress, Povolo and Hermida (Povolo and Hermida, 1995; Povolo et al., 1996) proposed a linear dependence of the internal stress with temperature, but they do not have a physical model that can explain it. Nonetheless, we believe that the linear dependence of σ_i can find some justification in the work of Rault (1998). This author applied the compensation law to the yielding of amorphous and semi-crystalline polymers. Accordingly, the yield stress may be written as:

$$\sigma_y = \sigma_0 - \frac{\sigma_0}{T_g} T + \frac{kT}{V} \ln \frac{\dot{\varepsilon}}{\dot{\varepsilon}_0} \tag{9}$$

where σ_0 may be associated with the athermal stress $\sigma_i(0)$ of the cooperative model. If Eqs. (5) and (9) are compared, it can be seen that the first term of both yield stress models exhibits a linear dependence on temperature. As mentioned by Rault (1998), the ratio σ_0/T_g is found to be on the order of 0.5 MPa/K for many thermoplastic polymers. This value is in good agreement with the cooperative model, since we recently found $m \approx 0.5$ MPa/K for three amorphous polymers (Richeton et al., 2005).

5. Results and discussion for the yield stress

In considering the deformation of polymers, the yield stress is generally defined as the true stress at the peak value on the stress–strain curves, and this definition is used herein. We remind the reader that the quasi-static tests were made at a constant crosshead speed, which does not provide a constant strain rate during loading at large strains. However, the strain rate variation occurring before yielding (small strains) has a negligible effect on the measured yield stress value.

5.1. Identification of the model parameters

The number of the parameters for the cooperative model is six (n, V, $\dot{\varepsilon}_0$, ΔH_β, $\sigma_i(0)$ and m). To identify these parameters, a reference temperature, T_{ref}, first has to be chosen. A reference temperature of 25 °C was chosen for all three polymers. Then a master curve of the experimental data has to be built at T_{ref} by using an Eyring plot representation (σ_y/T versus $\log \dot{\varepsilon}$). The horizontal and vertical shifts are determined to obtain the most suitable master curve. For the cooperative model, we have previously shown that the horizontal and vertical shifts can be expressed as (Richeton et al., 2005):

$$\begin{cases} \Delta(\log \dot{\varepsilon}) = \dfrac{\Delta H_\beta}{k \ln 10} \left(\dfrac{1}{T} - \dfrac{1}{T_{ref}} \right) \\ \Delta\left(\dfrac{\sigma_y}{T}\right) = -\sigma_i(0) \left(\dfrac{1}{T} - \dfrac{1}{T_{ref}} \right) \end{cases} \tag{10}$$

where ΔH_β and $\sigma_i(0)$ are the two adjusting parameters to get the most suitable master curve. In addition, the experimental data shifted horizontally and vertically have to satisfy the following equation:

$$\frac{\sigma_y}{T_{ref}} = \frac{\sigma_i(T_{ref})}{T_{ref}} + \frac{2k}{V}\sinh^{-1}\left(\frac{\dot{\varepsilon}}{\dot{\varepsilon}^*(T_{ref})}\right)^{1/n} \tag{11}$$

This equation is simply a rewriting of Eq. (2) for T_{ref}. The next step for the identification consists of calculating numerically the variables n, V, $\dot{\varepsilon}^*(T_{ref})$ and $\sigma_i(T_{ref})$ using a curve-fitting software to obtain the best fit of the shifted experimental data. The two remaining parameters $\dot{\varepsilon}_0$ and m derive directly from Eq. (4) taken at T_{ref}.

Fig. 5 represents the master curves of the experimental data built at 25 °C for PC, PMMA and PAI versus the corresponding numerical fits. The excellent agreement between the experimental data and the modeling validates the strain rate/temperature superposition principle for the reduced yield stress. The

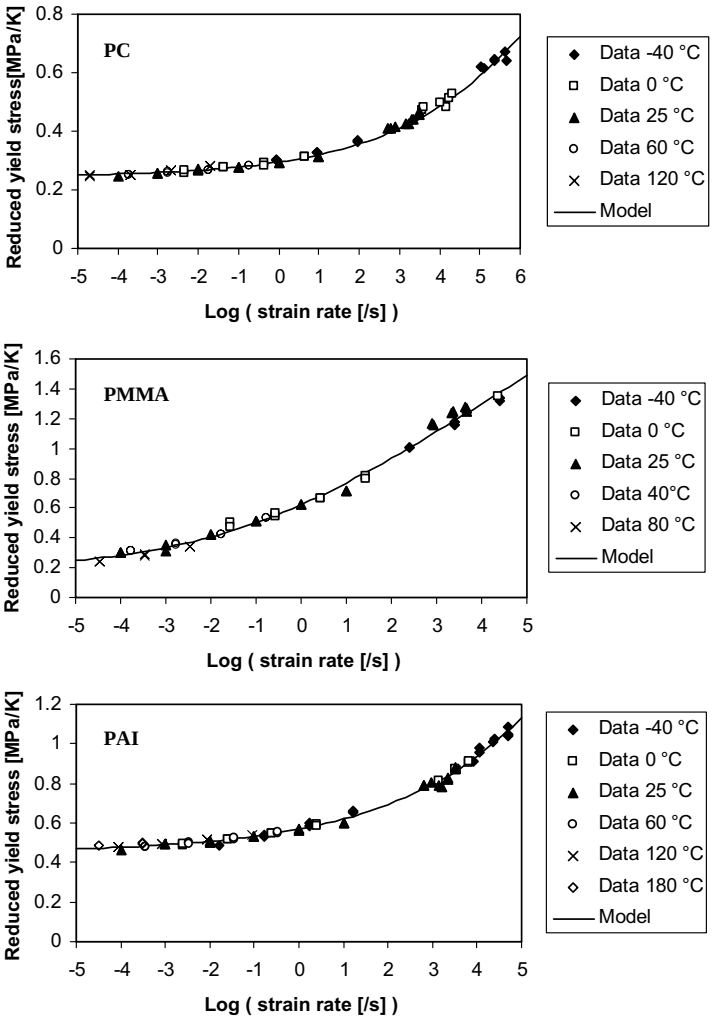

Fig. 5. Master curves built at 25 °C for PC, PMMA and PAI tested in uniaxial compression.

parameters used for the modeling can be found in Table 1. These parameters are in conformity with our preceding work (Richeton et al., 2005). The activation volume, V, is in the order of 10^{-29} m^3, the pre-exponential strain rate, $\dot{\varepsilon}_0$, is roughly in the same order as the Debye frequency (10^{12}–10^{14} Hz), the β activation energy, ΔH_β, is in the same range as those found in the literature for PC and PMMA, and the relation $m \approx \sigma_i(0)/T_g$ is quite well verified.

5.2. Strain rate dependence

Fig. 6 shows, for PC, PMMA and PAI, a comparison of the strain rate dependence for the compressive yield stress between the cooperative model and experimental data. The cooperative model shows good agreement with the data for different strain rates at different temperatures. This result further justifies our assumption concerning the strain rate/temperature superposition principle.

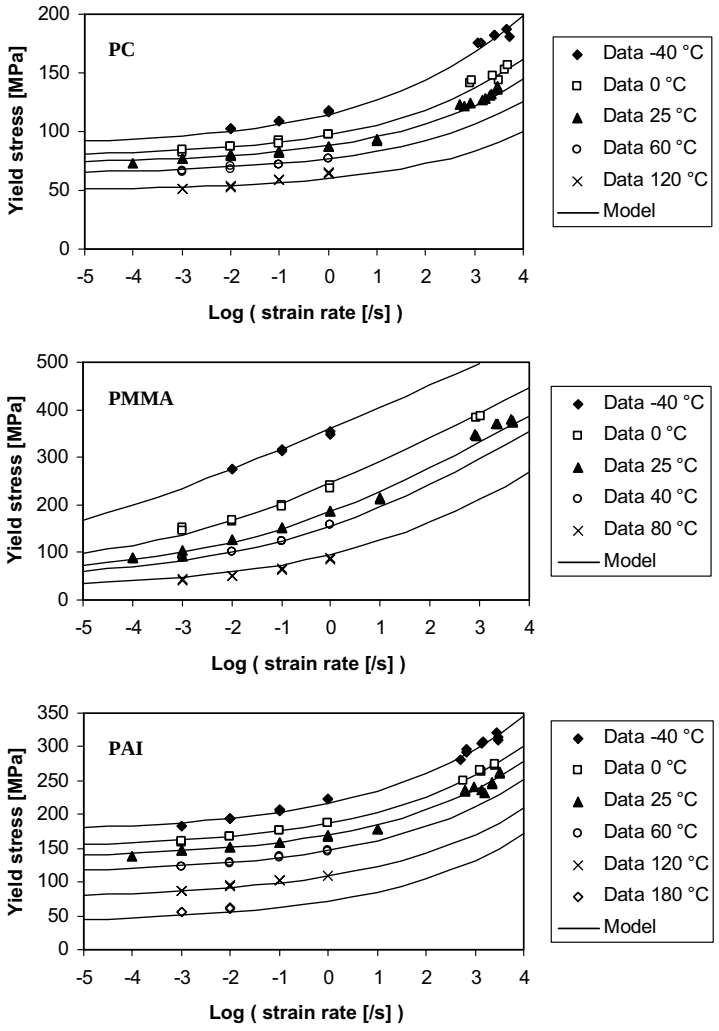

Fig. 6. Strain rate dependence of the compression yield stress for PC, PMMA and PAI.

For PC, the experimental data are comparable to what can be found in the article of Rietsch and Bouette (1990). At the low strain rates, PC displays a weak strain rate dependence, while at high strain rates, the yield stress increases dramatically with increasing strain rate.

For PMMA, the experimental data are qualitatively in agreement with the work of Bauwens-Crowet (1973). The modeling results are satisfactory in comparison with the experimental yield stress. Some data are missing for the lowest temperatures at the high strain rates. The reason is that PMMA is brittle under these conditions and breaks before reaching the yield point. The high strain rates results presented in this study strongly indicate that the cooperative model can be used for the modeling of the yield stress of PMMA at high strain rates; the master curve of Fig. 5 further supports the physics of the cooperative model.

For PAI, the model results are in good agreement with the experimental data. It can be noticed that the strain rate dependence of the yield stress of this material exhibits a behavior closer to PC than to PMMA. For the low strain rates, the yield stress of PAI is weakly dependent on strain rate. We believe that this observation implies that the β transition of PAI occurs at a very low temperature. Unfortunately, for this material, we do not find any values in the literature concerning the β activation energy or the β transition temperature. It will be very interesting to know if the activation energy given in Table 1 can be assimilated as the β activation energy of PAI determined by mechanical dynamical spectroscopy for example.

5.3. Temperature dependence

Concerning the temperature dependence of the compressive yield stress, the results for PC PMMA, PAI can be found in Fig. 7. The results are only presented at the strain rate of 0.01 s^{-1} to facilitate interpretation of the figures. The modeling results are in good agreement with the experimental data. Identical temperature dependence can be observed for other strain rates with the same satisfaction towards model predictions. As explained previously, the parameters were obtained based on the experimental data of the yield stress plotted as function of the strain rate. Consequently, it is quite remarkable that the same parameters can be used to correctly describe yield stress data plotted as function of temperature. This observation is another validation of the strain rate/temperature superposition principle.

For PC, the results are in agreement with those reported by Boyer (1968). At −100 °C, the yield begins to exhibit the appearance of the secondary transition. Extending the model to lower temperatures would result in a dramatic increase in yield stress, similar to that observed at high strain rates. PC also exhibits a sharp drop of the yield stress in the glass transition domain. This jump is due to the fact that the internal stress σ_i is not continuous through the glass transition. Nevertheless, the agreement between the modeling and experimental results remains good.

For PMMA, our experimental data are qualitatively in agreement with the work of Bauwens-Crowet (1973). The physics of the cooperative model is able to depict the mechanical behavior in the secondary transition region, in particular the shape of the curves for low temperatures. For temperatures far below −50 °C, the model cannot be applied anymore since no yield stress is observed in this temperature region due to brittle fracture. For temperatures above T_g, the model as given by Eq. (8) describes fairly well the mechanical behavior. Similar to the case for PC, this result is significant since it gives a better description than simply extrapolating Eq. (5) to the glass transition region. Moreover the yield stress given by the cooperative model vanishes towards the zero value for the $T > T_g$ temperatures, whereas the extrapolation of Eq. (5) would result in negative value for the absolute compressive yield stress at the very high temperatures.

For PAI, the calculated temperature dependence of the yield stress is linear down to low temperatures. This result suggests that the β transition of this material should occur below −100 °C. The lower the β transition, the more linear is the yield stress dependence on temperature at low temperatures. Unfortunately, we

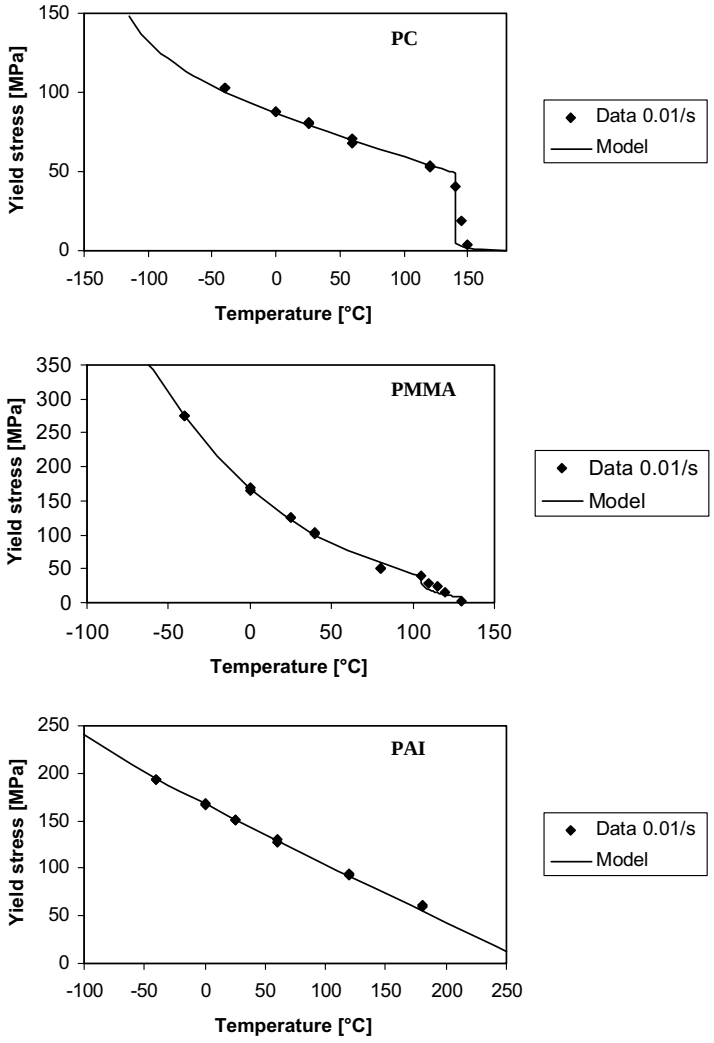

Fig. 7. Temperature dependence of the compression yield stress for PC, PMMA and PAI.

did not conduct tests below −100 °C, and therefore could not determine whether the material is still ductile in this temperature range. In addition, the cooperative model was not extrapolated above T_g due to the lack of experimental data, and because the WLF parameters of PAI are not known.

5.4. Effect of hydrostatic pressure

The parameters given in Table 1 are only valid for compression tests, and cannot be used directly to describe the tensile yield stress. The compressive yield stress of amorphous polymers is generally 15% higher than the tensile yield stress. This phenomenon is related to the fact that the hydrostatic pressure is positive in a compression test and negative in a tension test. The pressure sensitivity of polymers was observed by Rabinowitz et al. (1970) and by Spitzig and Richmond (1979). Their studies have shown that the yield stress exhibits a phenomenological linear dependence with applied pressure P:

$$\sigma_y(P) = \sigma_y(0) + \alpha_p P \tag{12}$$

where $\sigma_y(P)$ is the yield stress at pressure P, $\sigma_y(0)$ is the yield stress under zero pressure and α_p is a pressure sensitivity coefficient. From this latter development and according to the work of Boyce et al. (1988), the pressure dependence of the cooperative model can be expressed by:

$$\sigma_y = \tilde{\sigma}_i(0) - \tilde{m}T + \frac{2kT}{\widetilde{V}}\sinh^{-1}\left(\frac{\dot{\varepsilon}}{\dot{\varepsilon}^*(T)}\right)^{1/n} + \alpha_p P \tag{13}$$

Here σ_y is the yield stress independent of the mode of testing with the corresponding parameters $\tilde{\sigma}_i(0)$, $\tilde{m}$ and $\widetilde{V}$ (see Eq. (2)). In the absence of external pressure, P is the hydrostatic pressure defined by:

$$P = -\tfrac{1}{3}\mathrm{Trace}(\boldsymbol{\sigma}) \tag{14}$$

where $\boldsymbol{\sigma}$ is the stress tensor. For uniaxial compression tests, P is equal to $\sigma_y^c/3$ (σ_y^c is the absolute value of the compressive yield stress), whereas for tensile tests, P is equal to $-\sigma_y^t/3$ (σ_y^t is the tensile yield stress). By using Eq. (13), a system of two equations can be written:

$$\begin{cases} \left(1 - \dfrac{\alpha_p}{3}\right)\sigma_y^c = \tilde{\sigma}_i(0\ \mathrm{K}) - \tilde{m}T + \dfrac{2kT}{\widetilde{V}}\sinh^{-1}\left(\dfrac{\dot{\varepsilon}}{\dot{\varepsilon}^*(T)}\right)^{1/n} & \text{(a)} \\ \left(1 + \dfrac{\alpha_p}{3}\right)\sigma_y^t = \tilde{\sigma}_i(0\ \mathrm{K}) - \tilde{m}T + \dfrac{2kT}{\widetilde{V}}\sinh^{-1}\left(\dfrac{\dot{\varepsilon}}{\dot{\varepsilon}^*(T)}\right)^{1/n} & \text{(b)} \end{cases} \tag{15}$$

By equating the left hand side of Eq. (15a) with that of Eq. (15b), the pressure sensitivity coefficient α_p is obtained as:

$$\alpha_p = 3\frac{\sigma_y^c - \sigma_y^t}{\sigma_y^c + \sigma_y^t} \tag{16}$$

The numerical values of α_p can be calculated by testing the polymer in tension and in compression under the same temperature and strain rate conditions. For PC, α_p is equal to 0.08 after Boyce and Arruda (1990), for PMMA, α_p is set equal to 0.26 from Arruda et al. (1995), and for PAI, we found α_p equal to 0.43 with $\sigma_y^c = 165$ MPa and $\sigma_y^t = 124$ MPa (values found on www.matweb.com). Fig. 8 plots the experimental values of the pressure sensitivity coefficient α_p versus the temperature sensitivity parameter, m, along with the prediction of this relationship from the cooperative model. It is interesting to note that we found a linear relation between the pressure sensitivity coefficient α_p and the temperature sensitivity parameter m of the cooperative model for four amorphous polymers (Fig. 8). At the present time, we do not clearly understand

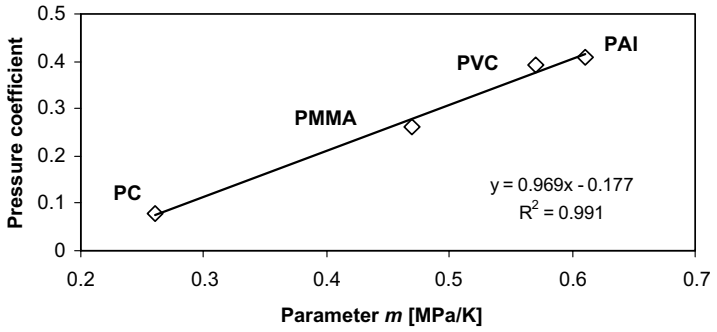

Fig. 8. Evidence of the linear relation between the pressure sensitivity coefficient α_p and the temperature sensitivity parameter m of the cooperative model. In the case of PVC, α_p is derived according to the work of Bauwens (1970) and m is given by Richeton et al. (2005).

the reason for this linear relation. Nonetheless, since there is an equivalence principle between strain rate and temperature, it could also be envisaged that there is an equivalence principle between pressure and temperature as well.

Furthermore, the parameters $\tilde{\sigma}_i(0)$, $\tilde{m}$ and $\widetilde{V}$, which are independent of the mode of testing (tension or compression) can be derived from the compression parameters and from the value of α_p. By comparing Eqs. (2) and (15a), we have:

$$\begin{cases} \tilde{\sigma}_i(0) = (1 - \alpha_p/3)\sigma_i(0) \\ \tilde{m} = (1 - \alpha_p/3)m \\ \widetilde{V} = \dfrac{1}{(1 - \alpha_p/3)} V \end{cases} \tag{17}$$

In fact, the numerical values of the parameters $\sigma_i(0)$, m and V determined for compression already included implicitly the effect of hydrostatic pressure. This result is significant since the cooperative model, as given in Eq. (13), should therefore be able to model both the compressive and tensile yield stresses. In particular, to derive the tensile yield stress from the compressive yield stress, Eq. (16) can be rewritten as:

$$\sigma_y^t = \frac{1 - \alpha_p/3}{1 + \alpha_p/3} \sigma_y^c \tag{18}$$

Nevertheless, this formula has to be used carefully, since the pressure coefficient α_p can only be regarded as a constant in the first order. In the work of Quinson et al. (1997), pressure coefficients have been found to depend slightly on temperature. To our knowledge no specific work has been made on the strain rate dependence. Nevertheless, the high strain rate results in tension and compression of Chen et al. (2002) tend to indicate that α_p is sensitive to the strain rate, due to the significant difference between quasi-static and dynamic responses observed.

6. Conclusions

The mechanical response of amorphous polymers is strongly affected by strain rate and temperature. In particular, the initial Young's modulus, the yield stress, and the strain hardening rate exhibit similar dependency on strain rate and temperature. An increase in temperature will decrease these quantities, whereas an increase of strain rate will increase these quantities. Moreover in this article, a new formulation of the cooperative model, as proposed by Richeton et al. (2005), for the description of the yield stress has been found to be capable of depicting the experimental results for a wide range of temperatures and strain rates, including the glass transition region as well as dynamic loadings. The physical nature of the cooperative model can definitely be seen as a first step toward the development of advanced material constitutive models for the description of the mechanical behavior of thermoplastic polymers for a wide range of temperature, strain rate and pressure.

Acknowledgments

This work was partially supported by the "*French National Centre for Scientific Research (CNRS)*" and the "*Région Alsace*" for the Ph.D. thesis of J. Richeton. In addition J. Richeton greatly appreciates the excellent work conditions and hospitality during his stay (summer 2004) at the Department of Mechanical and Aerospace Engineering at the University of California, San Diego.

References

Argon, A.S., 1973. A theory for the low temperature plastic deformation of glassy polymers. Philosophical Magazine 28, 839–865.

Arruda, E.M., Boyce, M.C., Jayachandran, R., 1995. Effects of strain rate, temperature and thermomechanical coupling on the finite strain deformation of glassy polymers. Mechanics of Materials 19, 193–212.

Bauwens, J.C., 1970. Yield condition and propagation of Lüder's lines in tension–torsion experiments on poly(vinyl chloride). Journal of Polymer Science: Part A-2 8, 893–901.

Bauwens, J.C., 1972. Relation between the compression yield stress and the mechanical loss peak of bisphenol-A-polycarbonate in the β transition range. Journal of Materials Science 7, 577–584.

Bauwens, J.C., Bauwens-Crowet, C., Homès, G., 1969. Tensile yield-stress behavior of poly(vinyl chloride) and polycarbonate in the glass transition region. Journal of Polymer Science: Part A-2 7, 1745–1754.

Bauwens-Crowet, C., 1973. The compression yield behaviour of polymethyl methacrylate over a wide range of temperatures and strain-rates. Journal of Materials Science 8, 968–979.

Bauwens-Crowet, C., Bauwens, J.C., Homès, G., 1969. Tensile yield-stress behavior of glassy polymers. Journal of Polymer Science: Part A-2 7, 176–183.

Bauwens-Crowet, C., Bauwens, J.C., Homès, G., 1972. The temperature dependence of yield of polycarbonate in uniaxial compression and tensile tests. Journal of Materials Science 7, 176–183.

Blumenthal, W.R., Cady, C.M., Gray III, G.T., 2002. Influence of temperature and strain rate on the compressive behavior of PMMA and polycarbonate polymers, shock compression of condensed matter-2001. In: Furnish, M.D., Thadhani, N., Horie, Y. (Eds.), AIP Conf. Proc. American Institute of Physics Press, Woodbury, New York, pp. 665–668.

Bowden, P.B., Raha, S., 1974. A molecular model for yield and flow in amorphous glassy polymers making use of a dislocation analogue. Philosophical Magazine 29, 149–166.

Boyce, M.C., Arruda, E.M., 1990. An experimental and analytical investigation of the large strain compressive and tensile response of glassy polymers. Polymer Engineering and Science 30, 1288–1298.

Boyce, M.C., Parks, D.M., Argon, A.S., 1988. Large inelastic deformation of glassy polymers. Part I: Rate dependent constitutive model. Mechanics of Materials 7, 15–33.

Boyer, R.F., 1968. Dependence of mechanical properties on molecular motion in polymers. Polymer Engineering and Science 8, 161–185.

Briscoe, B.J., Nosker, R.W., 1985. The flow stress of high density polyethylene at high rates of strain. Polymer Communications 26, 307–308.

Brulé, B., Halary, J.L., Monnerie, L., 2001. Molecular analysis of the plastic deformation of amorphous semi-aromatic polyamides. Polymer 42, 9073–9083.

Cady, C.M., Blumenthal, W.R., Gray III, G.T., Idar, D.J., 2003. Determining the constitutive response of polymeric materials as a function of temperature and strain rate. Journal de Physique IV France 110, 27–32.

Chen, L.P., Yee, A.F., Moskala, E.J., 1999. The molecular basis for the relationship between the secondary and mechanical properties of a series of polyester copolymer glasses. Macromolecules 32, 5944–5955.

Chen, W., Lu, F., Cheng, M., 2002. Tension and compression tests of two polymers under quasi-static and dynamic loading. Polymer Testing 21, 113–121.

Chou, S.C., Robertson, K.D., Rainey, J.H., 1973. The effect of strain rate and heat developed during deformation on the stress–strain curve of plastics. Experimental Mechanics 13, 422–432.

Eyring, H., 1936. Viscosity, plasticity, and diffusion as examples of absolute reaction rates. Journal of Chemical Physics 4, 283–291.

Ferry, J.D., 1980. Viscoelastic Properties of Polymers, third ed. John Wiley & Sons, New York.

Fotheringham, D., Cherry, B.W., 1976. Comment on "The compression yield behaviour of polymethyl methacrylate over a wide range of temperatures and strain-rates". Journal of Materials Science 11, 1368–1370.

Fotheringham, D.G., Cherry, B.W., 1978. The role of recovery forces in the deformation of linear polyethylene. Journal of Materials Science 13, 951–964.

Gray III, G.T., 2000. Classic split-Hopkinson pressure bar technique. In: Kuhn, H., Medlin, D. (Eds.), ASM—Handbook Volume 8 "Mechanical Testing and Evaluation". ASM International, Metals Park, OH, pp. 462–476.

Gray III, G.T., Blumenthal, W.R., 2000. Split-Hopkinson pressure bar testing of soft materials. In: Kuhn, H., Medlin, D. (Eds.), ASM—Handbook Volume 8 "Mechanical Testing and Evaluation". ASM International, Metals Park, OH, pp. 488–496.

Halary, J.L., Oultache, A.K., Louyot, J.F., Jasse, B., Sarraf, T., Muller, R., 1991. Viscoelastic properties of styrene-co-methyl methacrylate random copolymers. Journal of Polymer Science: Part B 29, 933–943.

Haward, R.N., Thackray, G., 1968. The use of a mathematical model to describe isothermal stress–strain curves in glassy thermoplastics. Proceedings of the Royal Society of London A 302, 453–472.

Kastelic, J.R., Baer, E., 1973. Crazing, yielding, and fracture in polycarbonate and polyethylene terephthalate at low temperatures. Journal of Macromolecular Science B 7, 679–703.

Kolsky, H., 1949. An investigation of the mechanical properties of materials at very high rates of loading. Proceedings of the Royal Society of London B 62, 676–700.

Povolo, F., Hermida, E.B., 1995. Phenomenological description of strain rate and temperature-dependent yield stress of PMMA. Journal of Applied Polymer Science 58, 55–68.

Povolo, F., Schwartz, G., Hermida, E.B., 1996. Temperature and strain rate dependence of the tensile yield stress of PVC. Journal of Applied Polymer Science 61, 109–117.

Quinson, R., Perez, J., Rink, M., Pavan, A., 1997. Yield criteria for amorphous polymers. Journal of Materials Science 32, 1371–1379.

Rabinowitz, S., Ward, I.M., Parry, J.S.C., 1970. The effect of hydrostatic pressure on the shear yield behaviour of polymers. Journal of Materials Science 5, 29–39.

Rana, D., Sauvant, V., Halary, J.L., 2002. Molecular analysis of yielding in pure and antiplasticized epoxy-amine thermosets. Journal of Materials Science 37, 5267–5274.

Rault, J., 1998. Yielding in amorphous and semi-crystalline polymers: the compensation law. Journal of Non-Crystalline Solids 235–237, 737–741.

Richeton, J., Ahzi, S., Daridon, L., Rémond, Y., 2003. Modeling of strain rates and temperature effects on the yield behavior of amorphous polymers. Journal de Physique IV France 110, 39–44.

Richeton, J., Ahzi, S., Daridon, L., Rémond, Y., 2005. A formulation of the cooperative model for the yield stress of amorphous polymers for a wide range of strain rates and temperatures. Polymer 46, 6035–6043.

Rietsch, F., Bouette, B., 1990. The compression yield behaviour of polycarbonate over a wide range of strain rates and temperatures. European Polymer Journal 26, 1071–1075.

Robertson, R.E., 1966. Theory for the plasticity of glassy polymers. The Journal of Chemical Physics 44, 3950–3956.

Roetling, J.A., 1965. Yield stress behaviour of poly(ethyl methacrylate) in the glass transition region. Polymer 6, 615–619.

Spitzig, W.A., Richmond, O., 1979. Effect of hydrostatic pressure on the deformation behavior of polyethylene and polycarbonate in tension and in compression. Polymer Engineering and Science 19, 1129–1139.

Walley, S.M., Field, J.E., Pope, P.H., Stafford, N.A., 1989. A study of the rapid deformation behaviour of a range of polymers. Philosophical Transactions of the Royal Society of London A 328, 1–33.

Xiao, C., Jho, J.Y., Yee, A.F., 1994. Correlation between the shear yielding behaviour and secondary relaxations of bisphenol A polycarbonate and related copolymers. Macromolecules 27, 2761–2768.